Atmos. Meas. Tech. Discuss., 3, 1399–1437, 2010
www.atmos-meas-tech-discuss.net/3/1399/2010/

Atmospheric Measurement Techniques Discussions

This discussion paper is/has been under review for the journal Atmospheric Measurement Techniques (AMT). Please refer to the corresponding final paper in AMT if available.

Continuous low-maintenance $CO_2/CH_4/H_2O$ measurements at the Zotino Tall Tower Observatory (ZOTTO) in Central Siberia

J. Winderlich[1], H. Chen[1], A. Höfer[1], C. Gerbig[1], T. Seifert[1], O. Kolle[1], C. Kaiser[2], J. V. Lavrič[1,2], and M. Heimann[1]

[1]Max Planck Institute for Biogeochemistry, Hans-Knöll-Straße 10, 07745 Jena, Germany
[2]Laboratoire des Sciences du Climat et de l'Environnement, Orme des Merisiers, 91191 Gif-sur-Yvette, France

Received: 22 March 2010 – Accepted: 23 March 2010 – Published: 31 March 2010

Correspondence to: J. Winderlich (jan.winderlich@bgc-jena.mpg.de)

Published by Copernicus Publications on behalf of the European Geosciences Union.

Abstract

The Zotino Tall Tower Observatory in Central Siberia (ZOTTO, 60°48′ N, 89°21′ E) is an excellent location to monitor the continental carbon cycle. Since April 2009, a fully automated low maintenance measurement system based on a cavity ring-down spectroscopy (CRDS) analyzer is installed at the site to measure continuously carbon dioxide (CO_2) and methane (CH_4) from six heights up to 301 m a.g.l. Buffer volumes in each air line remove short term CO_2 and CH_4 mixing ratio fluctuations associated with turbulence, and allow continuous, near-concurrent measurements from all six tower levels. Instead of drying the air sample, the simultaneously measured water vapor is used to correct the dilution and pressure-broadening effects for the accurate determination of dry air CO_2 and CH_4 mixing ratios. The stability of the water vapor correction was demonstrated by repeated laboratory and field tests. The effect of molecular adsorption in the wet air lines was shown to be negligible. The low consumption of four calibration tanks that need recalibration only on decadal timescale further reduces maintenance. The measurement precision (accuracy) of 0.04 ppm (0.09 ppm) for CO_2 and 0.3 ppb (1.5 ppb) for CH_4 is compliant with the WMO recommendations. The data collected during the 2009 vegetation period reveals a seasonal cycle amplitude of 26.4 ppm at the 301 m level.

1 Introduction

For the global climate, the most important greenhouse gases are water vapor (H_2O), carbon dioxide (CO_2) and methane (CH_4) (Kiehl et al., 1997). According to the IPCC Fourth Assessment Report (IPCC, 2007), CO_2 and CH_4 are the most important anthropogenic drivers of climate change: in 2005 the global mean mixing ratio was 379 µmol/mol (molar parts per million, ppm) CO_2 and 1774 nmol/mol (molar parts per billion, ppb) CH_4. For the understanding of the global carbon cycle the long term monitoring of sources and sinks of these two gases are indispensable. In particular

AMTD

3, 1399–1437, 2010

with regard to the spread in future climate projections, more investigation is needed to reduce the uncertainty in global coupled carbon cycle climate model simulations (Huntingford et al., 2009).

Atmospheric gas concentrations integrate the signal of exchange processes between land and ocean. Atmospheric measurements from observational networks have thus been used to infer surface-atmosphere exchange fluxes using inverse models (Gurney et al., 2002; Rödenbeck et al., 2003; Peylin et al., 2005). This so-called top-down approach has a high potential for providing meaningful carbon budgets on regional to continental scales. The atmospheric signal has particular advantages compared to measurements on plot level (e.g. from eddy covariance measurements), because it integrates the heterogeneous carbon release due to natural (fire, pests, windstorms) and anthropogenic disturbances (forest harvesting) (Körner, 2003). These disturbances primarily influence the human footprint in the carbon cycle of temperate and boreal forests (Magnani et al., 2007).

The localization of a supposed carbon sink on the Northern Hemisphere (Tans et al., 1990) needs further investigation. Different analytical methods such as remote sensing and inventory data (Schulze et al., 1999; Myneni et al., 2001), as well as the inversion models (Schimel et al., 2001; Gurney et al., 2002; Rödenbeck et al., 2003) suggest that a significant fraction of the Northern Hemisphere carbon sink is located in boreal forests. On the other hand, the region's wetlands are an important source of methane (Friborg et al., 2003). In future, a warmer climate with thawing permafrost makes microbial decomposition and fire disturbances more likely, which increases the carbon transfer to the atmosphere on decadal time scales (Schuur et al., 2008). Given the huge total estimate of 1672 Gt carbon stored in permafrost soils (Tarnocai et al., 2009), even small changes in the carbon fluxes could have a large potential impact on the global carbon cycle.

In the past, atmospheric measurement sites were mainly situated on remote coastal or mountain stations to suppress local disturbances for inverse model estimates of carbon sources and sinks. Terrestrial sites are difficult to incorporate into global models

(Rödenbeck et al., 2003), in particular because of the heterogeneous sources and sinks and the complex meteorological conditions close to the surface (Gerbig et al., 2003a; Gerbig et al., 2009). However, recent development in forward and inverse high resolution models show promising results to better integrate those sites in inversions (Peylin et al., 2005; Sarrat et al., 2007; Lauvaux et al., 2008; Trusilova et al., 2009).

Measurements from tall towers (>200 m) offer an opportunity to alleviate this difficulties: they provide access, at least during daytime, to the relatively well mixed planetary boundary layer (Stull, 1988) that is better represented in current global models and represents regions on larger scale than measurements closer to the ground (Gloor et al., 2001). During night time, in addition to sampling the stable boundary layer profile, tall towers often allow sampling of the residual layer air, whose gas concentrations correspond to those of the previous day.

Greenhouse gas measurements on tall towers have been pioneered in the 1990s in the United States (Bakwin et al., 1998) and in Hungary (Haszpra et al., 2001), and the network has been extended during the last decade in Europe (CHIOTTO project, Vermeulen, 2007). The Max Planck Institute for Biogeochemistry (MPI-BGC) equipped tall towers with CO_2, CH_4, CO, N_2O, and O_2/N_2 (and partly SF_6) measurements in Bialystok in Poland (Popa et al., 2010), near Zotino in Russia (Kozlova et al., 2008), and on top of the Ochsenkopf mountain in Germany (Thompson et al., 2009).

1.1 The ZOTTO Site

The Zotino Tall Tower Observatory (ZOTTO) is located in Central Siberia at 60°48′ N, 89°21′ E, approximately 20 km west of Zotino village at the Yenisei River (114 m a.s.l.). The ecosystem in the light taiga around the station comprises Pinus sylvestris forest stands on lichen covered sandy soils (Schulze et al., 2002). The closest large city Krasnoyarsk (950 000 inhabitants) is situated about 600 km south of the station. Two day lasting transport of equipment to this remote location is only possible in winter, implying an inherent need to reduce maintenance efforts and the consumption of consumables.

Siberian ecosystems are of major importance for future climate developments: they especially are projected to face increases in winter temperature and precipitation that feed back to the ecosystem (Bedritsky et al., 2008). Nevertheless, they are poorly covered with atmospheric measurement stations (e.g. GAW network). This lack will be reduced by long-term observations at the ZOTTO station. Additional stations are built up that focus mainly on South West Siberia such as the so-called 9-tower network (Arshinov et al., 2009a), and aircraft measurements are performed (Paris et al., 2008; Arshinov et al., 2009b).

A further argument for long-term measurements at ZOTTO is given by Lagrangian transport model STILT calculations (Gerbig et al., 2003b; Lin et al., 2003). The integrated surface influence of 5 days back trajectories based on ECMWF forecast data for the 2009 vegetation period is plotted in Fig. 1. Whereas the near field of the tower has the main influence, with one to two orders of magnitude reduced surface influence, the influence region covers about 1 000 000 km^2 of Central Siberia, slightly deformed towards the west in direction of the Ob swamplands and northwards along the Yenisei River. Thus, the ZOTTO footprint covers permafrost regions as well. Moreover, model simulations indicate a good signal to noise ratio especially in Central Siberia to detect changes in carbon fluxes in Eurasia with inverse methods (Karstens et al., 2006). Altogether, it proves ZOTTO as a good location to further investigate ecosystem functioning of the continental boreal region.

In the past, the ecosystems around ZOTTO were monitored for several years by aircraft (Lloyd et al., 2001, 2002; Styles et al., 2002) and Eddy covariance systems (Valentini et al., 2000; Röser et al., 2002; Shibistova et al., 2002). The construction of a new 304 m tall tower finished in September 2006 (Schulze et al., 2010). Aerosol and carbon monoxide measurements are done on 301 m and 52 m tower heights (Heintzenberg et al., 2008; Mayer et al., 2009); ozone and NO_x are analyzed from 30 m level (Vivchar et al., 2009). Until June 2007, a complex gas measurement system for CO_2, O_2, CH_4, CO, and N_2O based on gas chromatography, paramagnetic sensors, and near-infrared spectroscopy was operated providing trace gas information for five tower

levels (Kozlova et al., 2009). Replacing this complex system, we present in this paper the equipment of the site with a new low maintenance high precision CO_2/CH_4 measurement system that started operating in April 2009. In the subsequent sections we describe the detailed overall setup, validate the data, and present the first data series.

2 Experimental setup

2.1 Air flow diagram

The setup that allows selecting the air stream from one of the six tower levels (301 m, 227 m, 158 m, 92 m, 52 m, and 4 m a.g.l.) and transferring it to the gas analyzer is described in Fig. 2. A detailed part list is given in Table 1. The main part of the setup is situated in an air conditioned laboratory container within a measurement bunker at the base of the tower.

On the tower, the mushroom-shaped inlets (I1–I6) are equipped with 5 µm polyester filters. The relatively large surface of the ring shaped vent minimizes the possibilities of blocking the line, e.g. due to freezing in winter. All inlets are connected to 12 mm tubing (EATON Synflex 1300, Sertoflex), through which air is drawn to the measurement bunker at a flow rate of 15 l/min by piston pumps (CF1–CF6) to limit the time of air exchange in the lines, and to minimize wall effects.

In the measurement bunker a tee junction splits up the gas flow; a small amount of 150 standard cubic centimeters per minute (sccm) of air is extracted by the gas analyzer's internal pump from one tower level at a time. The air from all the lines not being analyzed is continuously purged at a flow rate of 150 sccm through a common line by a single purge pump (CP1) and controlled by a combination of needle valves (NV12–NV17) and flow meters (FM8–FM13) in order to assure similar conditioning of all lines.

The type of the needle valves (NV7–NV11) differs for each line, according to its flow characteristics. On the 301 m level line, no needle valve is used to minimize the

pressure drop; however, to avoid pressure fluctuations in the analyzer due to the motion of the pump piston, an additional air buffer volume is located upstream the flushing pump (CF1) for the 301 m line. The needle valves in all the other lines are chosen to match the pressure conditions in the 301 m line (~680 to 700 mbar).

Downstream, custom made 8 l stainless steel spheres act as buffer volumes on each sample line. They allow a continuous, near-concurrent measurement of six heights with only one single analyzer. While one line is analyzed, the others are continuously flushed with the same flow. Laboratory experiments have demonstrated the ideal mixing characteristic of the buffers. Consequently they integrate the air signal from every inlet with an e-folding time of approximately 37 min (8 l/150 sccm at 700 mbar, see also Sect. 3.5), bridging the time span between two consecutive measurements for each line.

To allow selective measurements of individual tower levels, 3-way solenoid valves V1–V6 are installed further downstream that switch the airflow between purge pump and analyzer. Those valves are characterized by easy to seal NPT threads, a big body orifice for minimal pressure drop, and small leak rates (<1 µl/s guaranteed). If the power supply of the valves and sensors fails, the measurement from 301 m is the default.

To select between measuring ambient air and calibration gases, the ambient air from the tall tower passes another two simultaneously switched 3-way solenoid valves V7–V8. For monitoring the analyzer's incoming air flow, a high quality, metal sealed, and well calibrated flow meter FM7 is installed. All flow meters in the setup are free of moving parts, thus requiring almost no maintenance and are, with the exception of flow meter FM7, not in contact with the analyzed air. The only active flow control of the whole system is performed by the analyzer itself.

In contrast to all tall tower instrumentation known to the authors, the pump of the analyzer is located downstream the measurement cell. This avoids an additional pump with its risk for leaks in the sampling line. The temperature corrected pressure record after an extensive, 25 h leak test showed leak rates less than 0.4 µl/s in all lines. Taking

AMTD
3, 1399–1437, 2010

a maximal observed CO_2 gradient of 1000 ppm in the laboratory container at 1 bar versus 300 ppm sample air at 0.7 bar, at the above leak rate the influence on the CO_2 concentration would be less than 0.02 ppm per line.

As there is no drying system, adsorption on additional large surfaces and potential leaks are excluded. The remaining maintenance efforts concentrate on regular annual pump maintenance, adjustments of needle valves to keep the pressure in all lines constant within a 650–700 mbar range, and annual filter cleanings.

2.2 The $CO_2/CH_4/H_2O$ analyzer

The CO_2, CH_4, and H_2O measurement is performed by an EnviroSense 3000i analyzer (Picarro Inc., USA, CFADS-17) based on the cavity ring-down spectroscopy technique (CRDS) (Crosson, 2008). The decay time of laser light inside a cavity equipped with highly reflective mirrors is measured for several wavelengths around 1.651 µm for CO_2 and H_2O (data output after ~4 s) and 1.603 µm for CH_4 (data output after ~1 s). The volume mixing ratios of the main isotopes $^{12}C^{16}O_2$, $^{12}C^{1}H_4$, and $^{1}H_2^{16}O$ are obtained by mathematical analysis of the spectral line shape. An outlet proportional valve controls the pressure and the temperature of the cavity to constant conditions of 187 mbar (140.0±0.04 Torr) and 40 000±0.004 °C. The mass flow of sample air through the cavity is linearly correlated with the inlet pressure (~150 sccm at 700 mbar).

Laboratory analyzer tests with humidified tank air (at 1.2% H_2O level) show a typical standard deviation of the raw data (0.2 Hz) below 0.06 ppm for CO_2, 0.5 ppb for CH_4, and 0.001% (10 ppm) for H_2O. To assess the long term stability of the analyzer, 200 h continuous measurement of air from a high-pressure tank was analyzed by the Allan variance technique (Allan, 1987), using "Alamath AlaVar 5.2" software. The continuous decrease of the Allan variance suggests that the chosen calibration interval of 100 h is fully sufficient.

Raw data from repeated measurements of calibration gas tanks have a long term drift of less than 0.25 ppm, and 3.2 ppb per year for CO_2 and CH_4, respectively.

The CRDS analyzer response is linear. The standard deviation of the residuals from the measurement data to the linear fit are 0.05 ppm and 0.05 ppb for a concentration range of 354–453 ppm CO_2, and 1804–2296 ppb CH_4.

The characteristic of the CRDS technology does not easily allow calibrations with air of non-natural composition. Experiments with synthetic air revealed residuals in the CO_2 calibration up to 1 ppm related to pressure broadening effects due to varying N_2, O_2 and Ar content in the calibration gases and the isotopic composition of CO_2 (Chen et al., 2010; Tohjima et al., 2009). To avoid problems, all our calibration tanks were filled with air of ambient isotopic composition. Even though the CRDS analyzer still detects only the main isotopes, there is no further isotope correction needed: the error that appears during the calibration emerges with the opposite sign during the measurement and thus cancels out. Measurement inaccuracies due to variations in the isotopic composition of ambient air ($\delta^{13}C_{VPDB}$=7.5–9.0‰, $\delta^{18}O_{VPDB}$=0.5–2.5‰) are too low to influence the measurement (<0.01 ppm at 400 ppm level) (Allison et al., 2007; Chen et al., 2010).

The H_2O measurement was calibrated using a dew point mirror (Dewmet, Michell instruments Ltd., UK) in the 0.7 to 3.0% H_2O range for another CRDS analyzer of the same type (model G1301-m, CFADS-30). Thus the actual values H_2O are calculated from the reported values H_2O_{CRDS} by the following formula (units in %):

$$H_2O = 0.0292 + 0.7719 \cdot H_2O_{CRDS} + 0.0197 \cdot H_2O_{CRDS}^2 \quad (1)$$

The nonlinear component is due to the self pressure broadening effect of water vapor.

Note that H_2O measurements from all CRDS analyzers have been calibrated to the same scale after production, so this formula also applies to the ZOTTO instrument.

2.3 Calibration system

To guarantee the required stability of the measurement, an automated calibration sequence is initialized every 100 h. The notional life time of the 200 bar high pressure tanks exceeds 60 years, but every 10 years a successive recalibration of the tanks is

suggested to exclude drifts in the mixing ratios and to adapt to the concentration range of the changing ambient air conditions.

The long usage time challenges the long term stability of the calibration gases. Therefore high pressure aluminum tanks are preferred to steel ones (Kitzis et al., 1999). However, the calibration gas composition can be changed through diffusive and surface processes (Langenfelds et al., 2005). High pressure tank regulators corrupt the gas concentration due to the long lasting storage, too (Da Costa et al., 1999). Life times of at least 12 years can be assured by careful gas handling like in tank calibrations, usage exclusively above 30 bar and pre-use regulator flushing procedures (Kitzis et al., 1999; Daube Jr. et al., 2002; Keeling et al., 2007).

To further reduce effects from the pressure regulators, polychlorotrifluoroethylene (PCTFE) is preferentially used as sealant to reduce gas permeation (Sturm et al., 2004). Our own laboratory experiments confirm the advantages of a PCTFE-equipped pressure regulator to suppress CO_2 corruption in the withdrawn air after storage (Winderlich, 2007). Additionally, the stability of the CO_2 concentration in tanks was observed to be better when they are stored in horizontal position (Keeling et al., 2007).

Hence, our calibration system consists of four horizontally stored aluminum tanks (50 l, Luxfer, C/O Matar, Italy) equipped with Ceodeux PCTFE cylinder valves (D 200 series, D20030163, Rotarex Deutschland GmbH, Germany), PCTFE sealed pressure regulators (RE1–RE4 in Fig. 2), and metal sealed high pressure transmitters (P8–P11).

As the analyzer has a linear response (Sect. 3.2), the three tanks of our setup are sufficient for the calibration. The fourth tank is used as target gas for quality control and further experiments. The CO_2 and CH_4 concentrations in the gas tanks that are currently used at ZOTTO (Table 2) were determined in the GASLAB of the MPI for Biogeochemistry Jena and are traceable to scales of the World Meteorological Organization (WMO) maintained in NOAA/ESRL (WMO-X2007 for CO_2, Zhao et al., 2006, NOAA-2004 for CH_4, Dlugokencky et al., 2005).

2.4 Water correction

Water influences the measurement of CO_2 and CH_4 by dilution and pressure broadening. At constant pressure in the optical cavity, dilution decreases the trace gas concentration linearly with increasing water vapor pressure, whereas pressure broadening is a nonlinear effect (Chen et al., 2010). For comparisons between different stations and for the use in atmospheric models, the dry mixing ratio is important, since wet mixing ratios show alterations just by changing water concentrations.

The analyzer already includes a first order water correction function:

$$\frac{CO_{2wet}}{CO_{2dry}} = 1 - 0.01244 \cdot H_2O_{CRDS}. \quad (2)$$

Experiments with a Licor LI-610 Humidifier revealed the necessity for a second order water correction function (Chen et al., 2010). The associated tests were performed for the CFADS-17 instrument in January 2009. A simpler setup had to be developed for ZOTTO, because the time-consuming laboratory experiments required a large amount of space, extensive flow regulations, and drift corrections due to temperature-dependent CO_2 dissolution in the water reservoir of the humidifier.

To humidify air, it suffices to pass it over a water droplet in a vessel (Frank Meinhardt and Rainer Schmitt, personal communication, 2008). The modified setup for the experiments in September 2009 is based on a stainless steel water trap with a volume of 19 cm^3 and an inner surface area of less than 140 cm^2 to reduce surface effects (Fig. 3a, adapted from Popa, 2007). The air from a high pressure tank flows through a dip-tube that almost touches a water droplet (< 1 ml) on the bottom of the trap. The humidified air leaves the trap through an outlet at its top. Because temperature changes of the trap to achieve different dew points resulted in unstable conditions, the trap was held at constant temperature within an ice bath, whereas the pressure of the flushing gas was changed: with decreasing absolute pressure, the relative amount of water vapor increases, even though the absolute water vapor content stays the same at constant temperature. For this freely controllable water vapor time series, the analyzer's

AMTD
3, 1399–1437, 2010

readings give CO_2 and CH_4 wet mixing ratios X_{wet} for a H_2O_{CRDS} range from 0 % to almost 4% (Fig. 3b).

The pressure variations trigger changes in the air adsorption processes at the metal surfaces of the trap. To ensure equilibration, data points 1.5 min before and 3 min after pressure changes are rejected (grey dots in Fig. 3b). Additionally, the required pressure stability of the CO_2/CH_4 measurement was confirmed experimentally since changing inlet pressure did not influence the instrumental reading of the mixing ratios above the internal sample cell pressure (187 mbar).

When the water droplet is completely evaporated, the analyzer detects the dry mixing ratio X_{dry} for CO_2 and CH_4 (red dots in Fig. 3b), and the water correction function can be directly inferred (Fig. 3c, d). The relation between H_2O content and the X_{wet}/X_{dry} ratio for CO_2 and CH_4 are fitted with a second order H_2O correction function:

$$\frac{X_{wet}}{X_{dry}} = 1 - a \cdot H_2O_{CRDS} - b \cdot H_2O_{CRDS}^2 \quad (3)$$

The experiments conducted in January and September 2009 are in good agreement, indicating temporal stability of the water correction function. The average fit parameters for both experiments are $a=(1.205\pm0.002)\cdot10^{-2}/\%$ and $b=(2.03\pm0.08)\cdot10^{-4}/\%^2$ for CO_2 and $a=(1.007\pm0.005)\cdot10^{-2}/\%$ and $b=(1.45\pm0.18)\cdot10^{-4}/\%^2$ for CH_4, while H_2O is given in percent. All raw data points (Fig. 3b) were grouped according to the set H_2O levels; thus only the binned and averaged CO_2 and CH_4 ratios are shown in Fig. 3c and d for better visibility.

Hence, the CO_2 accuracy better than 0.1 ppm relies on the water vapor measurement having the precision better than 200 ppm H_2O at a 400 ppm CO_2 level, which is easily achieved with the CRDS technique.

The standard deviation of the residuals of the individual fits indicates a repeatability of the water-corrected measurement within 0.03 ppm and 0.3 ppb for CO_2 and CH_4, respectively.

2.5 Influence of long inlet tubes

Although the analyzing system guarantees high quality data for moist ambient air samples, it has to be ensured, that the air sample remains unaltered on the way from the different tower inlets to the analyzer. The most important source of disturbances is assumed to be caused by water vapor. According concerns resulted in deploying air drying systems directly at the inlet of some towers (Vermeulen, 2007).

Here we try to evaluate the disturbances caused by water vapor in the inlet system. Due to the 300 mbar pressure drop in the 300 m inlet tube, the dew point is suppressed by 1 to 2 K per 100 m (dew point calculation based on H_2O saturation pressure from Goff equation, Murphy et al., 2005). Thus, condensation of water is highly unlikely which permits neglecting liquid water in our first order estimates.

We set up two CRDS analyzers (CFCDS-3 and CFADS-14) to measure ambient air simultaneously through a 2 m and a 200 m tube (1/2″ Dekabon). The 200 m tube was stored outside (winter days, temperature −1 to 5 °C, relative humidity 79 to 98%). The inlets of both lines were closely attached to each other. The data was recorded in 60 s averages, corrected for dilution and pressure broadening by water (see Sect. 3.3), and calibrated.

In our experiment, both instruments ran in parallel for three days. Accounting for the time delay, the linear interpolated 200 m data was time shifted by 1683 s. Thereafter it differed from the 2 m line by −(0.03±0.24) ppm CO_2, −(0.27±0.59) ppb CH_4 (compare Fig. 4) during the entire test period.

To simulate the deployment of the 8 l buffer volumes, the time series were convoluted with an exponential function. Any condensation at the walls of the stainless steel buffers can be excluded due to the reduced dew point associated with the low pressure (≤700 mbar). Because a well mixed volume V with the concentration c_0 will respond to an incoming flow f and the concentration c_1 with a time-dependent function $c(t)$

$$c(t) = c_1 + (c_0 - c_1)e^{-t/\tau} \text{ with time constant } \tau = \frac{V}{f} \quad (4)$$

AMTD
3, 1399–1437, 2010

this function can be applied also to the buffer volumes (τ=37 min, see Sect. 3.1). The differences become less noisy: $-(0.03\pm0.04)$ ppm CO_2, $-(0.28\pm0.21)$ ppb CH_4.

This test accounts only for small flow rates of the analyzers (240 and 270 sccm). In ZOTTO the flushing of the tubes at a 60 times larger rate (15 l/min) will outweigh additional influences of the longer tube (300 m) and higher H_2O concentrations in summer. Hence, the influence of long tubing on the gas concentration measurement can be neglected.

2.6 Data acquisition

A custom-made LabVIEW program (National Instruments Germany GmbH) installed on a central measurement PC controls all switching processes, calibration cycles, and signal processing. A data acquisition card (PCI-6225) acts as central hardware interface, to read sensor voltages (together with SCB-68 I/O card), and to control the solenoid valves with a relay board (ER-16 SPDT; all made by National Instruments Germany GmbH). The central measurement PC is connected to the CRDS analyzer via serial RS232 cable.

For time synchronization of the different data sets collected on the site (meteorology, aerosols, CO), the measurement PC was equipped with a high quality time card (ClockCard PCI Pro, Beagle Software, USA) and was set as central time server for other instruments via internal Ethernet network.

Data points are recorded every 30 s, including the average from the raw data of the analyzer and the current reading of all sensors. Additionally, all one second raw data from the CO_2/CH_4 analyzer is archived. For each tower level six data points are recorded within 3 min. For data analysis, first three data points (1.5 min) are rejected. All 6 tower levels, starting at the top, are consecutively measured within 18 min.

The post-processing code is written with the R software (http://www.r-project.org/) and removes a few outliers that originate from sporadic malfunction of valve V5 (replaced in September 2009), maintenance interruptions, etc. Afterward, all data points are corrected for dilution and pressure broadening from water by applying a second

order function of 30 s averaged H_2O raw data to CO_2 and CH_4 data (see Sect. 3.3).

For CO_2 and CH_4 calibration, every 100 h each of the three calibration tanks is measured for 8 min. This time span generously allows the calibration gases to flush the pressure regulators and remove the wet ambient air from the part of the tubing used conjointly. The mean of the last four minutes gives the analysis values for the linear calibration curve (see Sects. 3.2 and 3.3). Between two calibrations, the fit parameters are linearly interpolated to account for the drift of the analyzer.

2.7 Flask sampling system

To provide information on a larger number of species (CO_2, CH_4, CO, N_2O, isotopes, etc.), to validate continuous measurements and to bridge potential breakdowns of the continuous analyzer, air samples are collected from the 301 m level in 1 l glass flasks twice a week; however the series has several interruptions lasting for several weeks to months due to transport shortages.

To remove the water vapor, the sampled air passes through a glass trap within a fridge at 2 to 5 °C and through two stainless steel traps cooled to −90 °C (Fig. 2). Prior to filling the flasks, the tower tubing is flushed at a flow rate of 2 l/min for 40 min to prevent adsorption from affecting gas concentrations. During filling, air is pumped at a flow of 2 l/min through three flasks for 15 min by an upstream compressor pump (KNF Neuberger GmbH, Germany, Type: PM22619-814). When a pressure of 13 psig (~900 mbar above ambient) is reached in the flasks, flushing of the flasks continues and the excess flow is released via an excess flow valve.

2.8 Meteorological measurements

Various meteorological instruments have been installed at ZOTTO station in the year 2007 (Table 3). They record meteorological variables in a vertical profile on the tower as well as a number of soil parameters in vertical and horizontal profiles at two locations about 100 m southeast from the tower. One soil parameter measurement site is located

within a densely wooded area (forest site), the other within a sparsely vegetated area (bare land site). At both places, the sandy soil is covered by lichens.

A scheme of the meteorological measurement setup, as well as the data handling and data distribution is shown in Fig. 5. The meteorological data acquisition can be divided in two independent systems.

One system consists of five CR10X dataloggers (Campbell Scientific Ltd., UK), controlled by the PakBus operating system (version 10). Four of the loggers collect the data remotely from the sensors at different sites (forest, bare land, tower at 5 m and 302 m a.g.l.). The two dataloggers on the ground record vertical profiles of soil temperature, soil moisture, and three soil heat flux plates each. One logger collects data from a rain gauge and measures total and diffuse photosynthetically active radiation (PAR). The dataloggers on the tower measure air temperature, humidity, and pressure, and also radiative fluxes in different spectral bands (short wave solar, long wave terrestrial and PAR) at 302 m. The fifth datalogger operates as master, regularly collecting all data from the remotes and acting as their time server. Finally, the meteorology laptop collects and stores the data from the master logger using LoggerNet software (Campbell Scientific Ltd., UK) and updates its clock.

The second system consists of six 3-D sonic anemometers mounted in a vertical profile along the tower. Temperature humidity sensors and pressure transducers are connected to the analogue input channels of the anemometers. Each anemometer is connected to the meteorology laptop, which collects all the data with customized software, stores it, and transfers it to the central measurement PC.

To survey the stability of the tower basement, a laser beam distance meter monitors the distance between the tower and the first guy wire foundation in northeast direction.

3 Results and discussion

3.1 Data quality assessment

The station was equipped with the new analyzing system in April 2009. Since 20 May 2009 the measurement is authorized by Russian FSTEC agency. Until 24 November 2009, the total time of missing data due to humidification experiments (Sect. 3.4), maintenance or malfunctions is limited to 72 h (1.5%).

To monitor the accuracy of the instrument, one target tank is measured every 200 h for 8 min randomly distributed between two calibration cycles, and is treated like ambient air measurement data. After applying the calibration procedure (Sect. 3.6), the measured CO_2 and CH_4 concentrations of the target tank are 404.34±0.04 ppm and 1947.4±0.3 ppb for the whole time period so far. A comparison with values from the Jena GASLAB in Table 2 (404.40±0.08 ppm/1947.4±1.4 ppb) indicates an adequate accuracy of the system for dry air measurements. The CO_2 measurement is slightly biased, but the deviation is still within the error limit of the Jena GASLAB calibration laboratory, thus statistically insignificant. Earlier calibrations of the CRDS system are highly repeatable, which indicates that the accuracy is limited by the noise of the laboratory calibration.

In conclusion the accuracy of the instrument is 0.09 ppm for CO_2 and 1.5 ppb for CH_4, if statistical independence between target tank measurement of the CRDS analyzer, calibration laboratory (Table 2), and H_2O correction (Sect. 3.4) is assumed.

We used the flask measurements to validate the continuous measurement data. The mean difference between the linear interpolation of the in situ 30 s data and currently all available flask data for the first month of measurements is (0.05±0.08) ppm for CO_2 and (1.0±0.8) ppb for CH_4. The results clearly fulfill the qualifications for WMO interlaboratory comparability (0.1 ppm for CO_2, 2 ppb for CH_4, GAW Report No.186, 2007) and underline the high quality of the data. The integrating effect of the air buffer volumes simplifies comparisons between continuous and flask measurements, avoiding

AMTD
3, 1399–1437, 2010

complex mathematical operations to harmonize highly variable in situ data with flask results representative for 0.5 min filling periods ($\tau = V/f = 1\,l/2\,l/min$).

3.2 CO_2, CH_4 and H_2O measurement series

The $CO_2/CH_4/H_2O$ measurement series from six tower levels covers the whole vegetation period in 2009. All data points of the 301 m level are plotted in Fig. 6a. The day time values during well-mixed conditions in the planetary boundary layer (14:00 to 17:00 local time zone) can be fitted by a 4th harmonic function, and reveal a seasonal cycle amplitude of 26.4 ppm. This number is in line with previous values of 26.6 ppm at ZOTTO in the year 2007 (Kozlova et al., 2008). The amplitude is more pronounced than at continental tall tower sites with stronger marine influence, e.g. Bialystok, Poland with 23 ppm (Popa, 2007), or even Ochsenkopf, Germany with 15.5 ppm (Thompson et al., 2009) at the uppermost tower levels (300 and 163 m a.g.l., respectively).

In contrast to CO_2, the CH_4 concentration has an almost flat baseline, which does not vary throughout the year (Fig. 6b) with concentration spikes during the vegetation period. They are most pronounced during July, when most biotic activity in the surrounding bogs takes place and forest fires occur.

The water vapor measurement was compared to the meteorological data series of air temperature and relative humidity. WMO recommends the Goff equation from 1957 to calculate the saturation water vapor according to air temperature (Murphy et al., 2005). The saturation water vapor is multiplied with relative humidity and pressure from the tower top level to receive absolute H_2O concentration from meteorology (Fig. 6c), which correlates well with the calibrated H_2O from the CRDS analyzer (Eq. 1): the slope is 1.03 (insignificant compared to 1.3% relative error in H_2O calibration and 2% uncertainty in relative Humidity measurement) and the correlation coefficient $R^2 = 0.99$. This procedure represents an independent check on the calibration, and validates the transfer of our laboratory tests with CFADS-30 (Sect. 3.2) to the CFADS-17 instrument deployed in ZOTTO.

The profiles of CO_2 and CH_4, given by the measurement at different height levels, as well as vertical tracer gradients provide information on trace gas fluxes at local to regional scales. The implemented air buffer volumes allow a quasi continuous measurement from all tower heights with only one instrument. Furthermore, they remove short term fluctuations from atmospheric turbulences; such fluctuations have for example been observed in the Bialystok time series of CO_2 at the 300 m top level (Popa et al., 2010), with a standard deviation of 3 min integrated samples over 40 min (our buffer integration time) amounting to 1.1 ppm during July 2009. This facilitates interpretation when using atmospheric transport models, which do not represent turbulence. As a side effect, the buffered, less variable data takes full advantage of the low-noise analyzer signal.

The combination of integrating buffer volumes and fast line to line switching enhances the representativeness of our data compared to other up-to-date tall tower data series. Usually a distinct diurnal cycle in CO_2 and CH_4 mixing ratios becomes visible on monthly averages only (e.g. July 2009, Fig. 7a), whereas it is revealed already on hourly timescales in our data, e.g. during the summer night from 22 to 23 July 2009 shown in Fig. 7b. Immediately after sunset, the ground cools faster than the overlaying air as it has a broader long wave radiation spectrum. Thus, the air in the lower 300 to 500 m stratifies to a stable nocturnal boundary layer (Stull, 1988). This inversion layer traps the emitted CO_2 and CH_4 during night. The closer to the ground the air parcel is located, the higher the concentration rises. As soon as the morning sun light warms the surface again (starting shortly before 06:00, Fig. 7), the air starts vertical mixing from the ground and the carbon that was trapped in the surface layer gets diluted with increasing air layer thickness. Thus, the concentration differences between adjacent tower heights fade away until they all reach the concentration of the well-mixed boundary layer during the day.

Combining these tracer gradients, the meteorological data, and prospective eddy covariance flux measurements with the information from footprint models render investigation of high resolution spatio-temporal flux patterns possible at the regional scale.

4 Summary and conclusions

In April 2009, the Zotino Tall Tower station was equipped with a CRDS analyzer to measure CO_2, CH_4, and H_2O in non-dried sample air. The H_2O measurement and the associated correction is temporally stable enough to guarantee a high quality of the CO_2 and CH_4 measurement and compares well to meteorological data. The water corrections on the CO_2 and CH_4 measurement were validated over a 9 month period with a simple experimental setup. The effect of molecular adsorption in the long air lines was investigated and shown to be negligible.

Regular target tank measurements reveal a precision of the instrument of 0.04 ppm for CO_2 and 0.3 ppb for CH_4. Adding measurement uncertainties of the calibration tanks and the water correction, the accuracy is 0.09 ppm CO_2 and 1.5 ppb CH_4. The difference between the continuous data and flask data is (0.05±0.08) ppm CO_2, and (1.0±0.8) ppb CH_4. This proves in an independent way that the accuracy of wet air measurements is compliant with the WMO requirements.

Without any drying system the maintenance is considerably reduced. Furthermore, the system sensors for diagnostic values (e.g. flow, pressure, etc.) are free of moving parts, which minimizes the possibility of failures. Calibration tanks will have to be recalibrated on a decadal timescale.

The data is temporally integrated by the use of buffer volumes in each air line, allowing a continuous, near-concurrent measurement from six heights. The 37 min integration time of each line suffices to bridge the 18 min period during which the analyzer is measuring other lines. The results are six smooth data series, which are not influenced by high frequency fluctuations associated with turbulent eddies. This allows a temporally highly resolved observation of the nocturnal boundary layer developments, thus enabling to better estimate local night time respiration. Additionally, footprint calculations confirm that the data from the tower's uppermost level will provide a valuable basis for future inverse modeling approaches for the central Siberian region.

AMTD
3, 1399–1437, 2010

Acknowledgements. The ZOTTO project is funded by the Max Planck Society through an International Science and Technology Center (ISTC) partner project no. 2757 within the framework of the proposal "Observing and Understanding Biogeochemical Responses to Rapid Climate Changes in Eurasia".

For servicing the installed setup at the ZOTTO station we deeply appreciate the work of A. Panov, A. Timokhina, A. Cukanov, and A. Sidorov from the Sukachev Institute of Forest in Krasnoyarsk. We also thank S. Verkhovets, V. Kislitsyn, the ZOTTO watchmen, and other supporters in Russia.

We thank E.-D. Schulze and M. Gloor for their efforts to build up the ZOTTO tower. We thank S. Schmidt for his travel support and drawing the plumbing diagram, and K. Kübler for his enormous efforts to maintain the station. Furthermore we thank A. Jordan who kindly provided the buffer volumes. We thank for the help of R. Thompson, U. Schultz, J. Steinbach, W. Brand, F. Voigt, B. Schlöffel, R. Leppert, M. Strube, M. Pittner, M. Hielscher, F. Hänsel, S. Baum and F.-T. Koch (MPI-BGC).

We thank A. van Pelt, C. Rella, and E. Crosson from Picarro Inc., USA for the immediate and comprehensive support.

The service charges for this open access publication
have been covered by the Max Planck Society.

References

Allan, D. W.: Time and Frequency (Time-Domain) Characterization, Estimation, and Prediction of Precision Clocks and Oscillators, IEEE T. Ultrason. Ferr., 34(6), 647–654, 1987.

Allison, C. E. and Francey, R. J.: Verifying Southern Hemisphere trends in atmospheric carbon dioxide stable isotopes, J. Geophys. Res.-Atmos., 112, D21304, doi:10.1029/2006jd007345, 2007.

Arshinov, M., Belan, B., Davydov, D., Inouye, G., Krasnov, O., Maksyutov, S., Machida, T., Fofonov, A., and Shimoyama, K.: Spatial and temporal variability of CO2 and CH4 concentrations in the surface atmospheric layer over West Siberia, Atmospheric and Oceanic Optics, 22(1), 84–93, doi:10.1134/S1024856009010126, 2009a.

Arshinov, M., Belan, B., Davydov, D., Inouye, G., Maksyutov, S., Machida, T., and Fofonov, A.: Vertical distribution of greenhouse gases above Western Siberia by the long-term measurement data, Atmospheric and Oceanic Optics, 22(3), 316–324, doi:10.1134/S1024856009030087, 2009b.

Bakwin, P. S., Tans, P. P., Hurst, D. F., and Zhao, C. L.: Measurements of carbon dioxide on very tall towers: results of the NOAA/CMDL program, Tellus, 50B(5), 401–415, doi:10.1034/j.1600-0889.1998.t01-4-00001.x, 1998.

Bedritsky, A. I., Blinov, V. G., Gershinkova, D. A., Golitsyn, G. S., Dymnikov, V. P., Izrael, Y. A., Kattsov, V. M., Kotlyakov, V. M., Meleshko, V. P., Osipov, V. I., and Semenov, S. M.: Assessment Report on Climate Change and its Consequences in Russian Federation - General Summary, Federal Service for Hydrometeorology and Environmental Monitoring (Roshydromet), Moscow, 24 pp., 2008.

Chen, H., Winderlich, J., Gerbig, C., Hoefer, A., Rella, C. W., Crosson, E. R., Van Pelt, A. D., Steinbach, J., Kolle, O., Beck, V., Daube, B. C., Gottlieb, E. W., Chow, V. Y., Santoni, G. W., and Wofsy, S. C.: High-accuracy continuous airborne measurements of greenhouse gases (CO_2 and CH_4) using the cavity ring-down spectroscopy (CRDS) technique, Atmos. Meas. Tech., 3, 375–386, 2010, http://www.atmos-meas-tech.net/3/375/2010/.

Crosson, E. R.: A cavity ring-down analyzer for measuring atmospheric levels of methane, carbon dioxide, and water vapor, Appl. Phys. B-Lasers O., 92(3), 403–408, doi:10.1007/s00340-008-3135-y, 2008.

Da Costa, G. and Steele, L. P.: Cape Grim's new low flow, high precision, in situ CO_2 analyser system - Development status and results from four month's operation at Aspendale, WMO 10. Meeting of Experts on CO_2 Measurements, Stockholm, 1999.

Daube Jr., B. C., Boering, K. A., Andrews, A. E., and Wofsy, S. C.: A High-Precision Fast-Response Airborne CO2 Analyzer for In Situ Sampling from the Surface to the Middle Stratosphere, J. Atmos. Ocean. Tech., 19, 1532–1543, doi:10.1175/1520-0426(2002)019<1532:AHPFRA>2.0.CO;2, 2002.

Dlugokencky, E. J., Myers, R. C., Lang, P. M., Masarie, K. A., Crotwell, A. M., Thoning, K. W., Hall, B. D., Elkins, J. W., and Steele, L. P.: Conversion of NOAA atmospheric dry air CH4 mole fractions to a gravimetrically prepared standard scale, J. Geophys. Res.-Atmos., 110(D18), D18306, doi:10.1029/2005JD006035, 2005.

Friborg, T., Soegaard, H., Christensen, T. R., Lloyd, C. R., and Panikov, N. S.: Siberian wetlands: Where a sink is a source, Geophys. Res. Lett., 30(21), 2129, doi:10.1029/2003GL017797, 2003.

GAW Report No.186: 14th WMO/IAEA Meeting of Experts on Carbon Dioxide, Other Greenhouse Gases and Related Tracers Measurement Techniques, Helsinki, Finland WMO TD No. 1487, 145 pp., 2007.

Gerbig, C., Lin, J. C., Wofsy, S. C., Daube, B. C., Andrews, A. E., Stephens, B. B., Bakwin, P. S., and Grainger, C. A.: Toward constraining regional-scale fluxes of CO_2 with atmospheric observations over a continent: 1. Observed spatial variability from airborne platforms, J. Geophys. Res.-Atmos., 108(D24), 4756, doi:10.1029/2002JD003018, 2003a.

Gerbig, C., Lin, J. C., Wofsy, S. C., Daube, B. C., Andrews, A. E., Stephens, B. B., Bakwin, P. S., and Grainger, C. A.: Toward constraining regional-scale fluxes of CO_2 with atmospheric observations over a continent: 2. Analysis of COBRA data using a receptor-oriented framework, J. Geophys. Res.-Atmos., 108(D24), 4757, doi:10.1029/2003JD003770, 2003b.

Gerbig, C., Dolman, A. J., and Heimann, M.: On observational and modelling strategies targeted at regional carbon exchange over continents, Biogeosciences, 6, 1949–1959, 2009, http://www.biogeosciences.net/6/1949/2009/.

Gloor, M., Bakwin, P. S., Hurst, D. F., Lock, L., Draxler, R., and Tans, P. P.: What is the concentration footprint of a tall tower?, J. Geophys. Res., 106(D16), 17831–17840, 2001.

Gurney, K. R., Law, R. M., Denning, A. S., Rayner, P. J., Baker, D., Bousquet, P., Bruhwiler, L., Chen, Y. H., Ciais, P., Fan, S., Fung, I. Y., Gloor, M., Heimann, M., Higuchi, K., John, J., Maki, T., Maksyutov, S., Masarie, K., Peylin, P., Prather, M., Pak, B. C., Randerson, J., Sarmiento, J., Taguchi, S., Takahashi, T., and Yuen, C. W.: Towards robust regional estimates of CO_2 sources and sinks using atmospheric transport models, Nature, 415(6872), 626–630, doi:10.1038/415626a, 2002.

Haszpra, L., Barcza, Z., Bakwin, P. S., Berger, B. W., Davis, K. J., and Weidinger, T.: Measuring system for the long-term monitoring of biosphere/atmosphere exchange of carbon dioxide, J. Geophys. Res., 106(D3), 3057–3069, doi:10.1029/2000jd900600, 2001.

Heintzenberg, J., Birmili, W., and Theiss, D.: The atmospheric aerosol over Siberia, as seen from the 300 m ZOTTO tower, Tellus, 60B, 276–285, doi:10.1111/j.1600-0889.2007.00335.x, 2008.

Huntingford, C., Lowe, J. A., Booth, B. B. B., Jones, C. D., Harris, G. R., Gohar, L. K., and Meir, P.: Contributions of carbon cycle uncertainty to future climate projection spread, Tellus, 61B(2), 355–360, doi:10.1111/j.1600-0889.2009.00414.x, 2009.

IPCC: Solomon, S., Qin, D., Manning, M., Alley, R. B., Berntsen, T., Bindoff, N. L., Chen, Z., Chidthaisong, A., Gregory, J. M., Hegerl, G. C., Heimann, M., Hewitson, B., Hoskins, B. J., Joos, F., Jouzel, J., Kattsov, V., Lohmann, U., Matsuno, T., Molina, M., Nicholls, N., Overpeck, J., Raga, G., Ramaswamy, V., Ren, J., Rusticucci, M., Somerville, R., Stocker, T. F., Whetton, P., Wood, R. A., and Wratt, D.: Technical Summary, in: Climate Change 2007: The Physical Science Basis, Contribution of Working Group I to the Fourth Assessment Report of the Intergovernmental Panel on Climate Change, edited by: Solomon, S., Qin, D., Manning, M., Chen, Z., Marquis, M., Averyt, K.B., Tignor, M., and Miller, H. L., Cambridge University Press, Cambridge, United Kingdom and New York, NY, USA, 2007.

Karstens, U., Gloor, M., Heimann, M., and Rödenbeck, C.: Insights from simulations with high-resolution transport and process models on sampling of the atmosphere for constraining midlatitude land carbon sinks, J. Geophys. Res., 111(D12), D12301, doi:10.1029/2005JD006278, 2006.

Keeling, R. F., Manning, A. C., and Paplawsky, W. J.: On the long-term stability of reference gases for atmospheric O_2/N_2 and CO_2 measurements, Tellus, 59B(1), 3–14, doi:10.1111/j.1600-0889.2006.00228.x, 2007.

Kiehl, J. T. and Trenberth, K. E.: Earth's annual global mean energy budget, B. Am. Meteorol. Soc., 78(2), 197–208, doi:10.1175/1520-0477(1997)078<0197:EAGMEB>2.0.CO;2, 1997.

Kitzis, D. and Zhao, C. L.: CMDL/Carbon Cycle Grennhause Gases Group Standards Preparation and Stability, in, U.S. Department of Commerce – National Oceanic and Atmospheric Administration (NOAA) – Climate Monitoring and Diagnostics Laboratory – Carbon Cycle Greenhouse Gases Group, http://www.cmdl.noaa.gov/ccgg/refgases/airstandard.html, last access: March 2010, 1999.

Körner, C.: Slow in, rapid out – Carbon flux studies and Kyoto targets, Science, 300(5623), 1242–1243, doi:10.1126/science.1084460, 2003.

Kozlova, E. A., Manning, A. C., Kisilyakhov, Y., Seifert, T., and Heimann, M.: Seasonal, synoptic, and diurnal-scale variability of biogeochemical trace gases and O_2 from a 300-m tall tower in central Siberia, Global Biogeochem. Cy., 22, GB4020, doi:10.1029/2008GB003209, 2008.

Kozlova, E. A. and Manning, A. C.: Methodology and calibration for continuous measurements of biogeochemical trace gas and O_2 concentrations from a 300-m tall tower in central Siberia, Atmos. Meas. Tech., 2, 205–220, 2009, http://www.atmos-meas-tech.net/2/205/2009/.

Langenfelds, R. L., van der Schoot, M. V., Francey, R. J., Steele, L. P., Schmidt, M., and Mukai, H.: Modification of air standard composition by diffusive and surface processes, J. Geophys. Res., 110, D13307, doi:10.1029/2004JD005482, 2005.

Lauvaux, T., Uliasz, M., Sarrat, C., Chevallier, F., Bousquet, P., Lac, C., Davis, K. J., Ciais, P., Denning, A. S., and Rayner, P. J.: Mesoscale inversion: first results from the CERES campaign with synthetic data, Atmos. Chem. Phys., 8, 3459–3471, 2008, http://www.atmos-chem-phys.net/8/3459/2008/.

Lin, J. C., Gerbig, C., Wofsy, S. C., Andrews, A. E., Daube, B. C., Davis, K. J., and Grainger, C. A.: A near-field tool for simulating the upstream influence of atmospheric observations: The Stochastic Time-Inverted Lagrangian Transport (STILT) model, J. Geophys. Res., 108(D16), 4493, doi:10.1029/2002JD003161, 2003.

Lloyd, J., Francey, R. J., Mollicone, D., Raupach, M. R., Sogatchev, A., Arneth, A., Byers, J. N., Kelliher, F. M., Rebmann, C., Valentini, R., Wong, S.-C., Bauer, G., and Schulze, E.-D.: Vertical profiles, boundary layer budgets, and regional flux estimates for CO_2 and its 13C/12C ratio and for water vapor above a forest/bog mosaic in central Siberia, Global Biogeochem. Cy., 15(2), 267–284, doi:10.1029/1999GB001211, 2001.

Lloyd, J. O. N., Langenfelds, R. L., Francey, R. J., Gloor, M., Tchebakova, N. M., Zolotuokhine, D., Brand, W. A., Werner, R. A., Jordan, A., Allison, C. A., Zrazhewske, V., Shibistova, O., and Schulze, E. D.: A trace-gas climatology above Zotino, central Siberia, Tellus B, 54(5), 749–767, doi:10.1034/j.1600-0889.2002.01335.x, 2002.

Magnani, F., Mencuccini, M., Borghetti, M., Berbigier, P., Berninger, F., Delzon, S., Grelle, A., Hari, P., Jarvis, P. G., Kolari, P., Kowalski, A. S., Lankreijer, H., Law, B. E., Lindroth, A., Loustau, D., Manca, G., Moncrieff, J. B., Rayment, M., Tedeschi, V., Valentini, R., and Grace, J.: The human footprint in the carbon cycle of temperate and boreal forests, Nature, 447(7146), 848–850, doi:10.1038/nature05847, 2007.

Mayer, J. C., Birmili, W., Heimann, M., Heintzenberg, J., Juergens, N., Kisilyakhov, Y., Panov, A., and Andreae, M. O.: Long-Term Measurements of Carbon Monoxide and Aerosols at the ZOTTO tall tower, Siberia, Eos Trans. AGU, Fall Meet. Suppl., Abstract GC31A-0686, 90(52), 2009.

Murphy, D. M. and Koop, T.: Review of the vapour pressures of ice and supercooled water for atmospheric applications, Q. J. Roy. Meteorol. Soc., 131(608), 1539–1565, doi:10.1256/qj.04.94, 2005.

Myneni, R. B., Dong, J., Tucker, C. J., Kaufmann, R. K., Kauppi, P. E., Liski, J., Zhou, L., Alexeyev, V., and Hughes, M. K.: A large carbon sink in the woody biomass of Northern forests, P. Natl. Acad. Sci. USA, 98(26), 14784–14789, doi:10.1073/pnas.261555198, 2001.

Paris, J. D., Ciais, P., Nedelec, P., Ramonet, M., Belan, B. D., Arshinov, M. Y., Golitsyn, G. S., Granberg, I., Stohl, A., Cayez, G., Athier, G., Boumard, F., and Cousin, J. M.: The YAK-AEROSIB transcontinental aircraft campaigns: new insights on the transport of CO_2, CO and O-3 across Siberia, Tellus B, 60(4), 551–568, doi:10.1111/j.1600-0889.2008.00369.x, 2008.

Peylin, P., Rayner, P. J., Bousquet, P., Carouge, C., Hourdin, F., Heinrich, P., Ciais, P., and AEROCARB contributors: Daily CO_2 flux estimates over Europe from continuous atmospheric measurements: 1, inverse methodology, Atmos. Chem. Phys., 5, 3173–3186, 2005, http://www.atmos-chem-phys.net/5/3173/2005/.

Popa, M. E.: Continuous tall tower multispecies measurements in Europe for quantifying and understanding land-atmosphere carbon exchange, PhD thesis, Chemisch-Geowissenschaftliche Fakultaet, Friedrich Schiller University Jena, 237 pp., 2007.

Popa, M. E., Gloor, M., Manning, A. C., Jordan, A., Schultz, U., Haensel, F., Seifert, T., and Heimann, M.: Measurements of greenhouse gases and related tracers at Bialystok tall tower station in Poland, Atmos. Meas. Tech., 3, 407–427, 2010, http://www.atmos-meas-tech.net/3/407/2010/.

Rödenbeck, C., Houweling, S., Gloor, M., and Heimann, M.: CO_2 flux history 1982–2001 inferred from atmospheric data using a global inversion of atmospheric transport, Atmos. Chem. Phys., 3, 1919–1964, 2003, http://www.atmos-chem-phys.net/3/1919/2003/.

Röser, C., Montagnani, L., Schulze, E. D., Mollicone, D., Kolle, O., Meroni, M., Papale, D., Marchesini, L. B., Federici, S., and Valentini, R.: Net CO_2 exchange rates in three different successional stages of the "Dark Taiga" of central Siberia, Tellus B, 54(5), 642–654, doi:10.1034/j.1600-0889.2002.01351.x, 2002.

Sarrat, C., Noilhan, J., Dolman, A. J., Gerbig, C., Ahmadov, R., Tolk, L. F., Meesters, A. G. C. A., Hutjes, R. W. A., Ter Maat, H. W., Pérez-Landa, G., and Donier, S.: Atmospheric CO_2 modeling at the regional scale: an intercomparison of 5 meso-scale atmospheric models, Biogeosciences, 4, 1115–1126, 2007, http://www.biogeosciences.net/4/1115/2007/.

Schimel, D. S., House, J. I., Hibbard, K. A., Bousquet, P., Ciais, P., Peylin, P., Braswell, B. H., Apps, M. J., Baker, D., Bondeau, A., Canadell, J., Churkina, G., Cramer, W., Denning, A. S., Field, C. B., Friedlingstein, P., Goodale, C., Heimann, M., Houghton, R. A., Melillo, J. M., Moore, B., Murdiyarso, D., Noble, I., Pacala, S. W., Prentice, I. C., Raupach, M. R., Rayner, P. J., Scholes, R. J., Steffen, W. L., and Wirth, C.: Recent patterns and mechanisms of carbon exchange by terrestrial ecosystems, Nature, 414(6860), 169–172, doi:10.1038/35102500, 2001.

Schulze, E. D., Lloyd, J., Kelliher, F. M., Wirth, C., Rebmann, C., Luhker, B., Mund, M., Knohl, A., Milyukova, I. M., Schulze, W., Ziegler, W., Varlagin, A. B., Sogachev, A. F., Valentini, R., Dore, S., Grigoriev, S., Kolle, O., Panfyorov, M. I., Tchebakova, N., and Vygodskaya, N. N.: Productivity of forests in the Eurosiberian boreal region and their potential to act as a carbon sink – a synthesis, Global Change Biology, 5(6), 703–722, doi:10.1046/j.1365-2486.1999.00266.x, 1999.

Schulze, E. D., Vygodskaya, N. N., Tchebakova, N. M., Czimczik, C. I., Kozlov, D. N., Lloyd, J., Mollicone, D., Parfenova, E., Sidorov, K. N., Varlagin, A. V., and Wirth, C.: The Eurosiberian Transect: an introduction to the experimental region, Tellus B, 54(5), 421–428, doi:10.1034/j.1600-0889.2002.01342.x, 2002.

Schulze, E. D., Vaganov, E. A., Gloor, M., Verkhovets, S. V., Manning, A. C., Heitzer, W., Endrullat, B., Radmacher, P., Kübler, K., Andeae, M. O., and Heimann, M.: A tall tower station for monitoring atmospheric greenhouse-gas concentrations in Central Siberia, Eos Trans. AGU, in preparation, 2010.

Schuur, E. A. G., Bockheim, J., Canadell, J. G., Euskirchen, E., Field, C. B., Goryachkin, S. V., Hagemann, S., Kuhry, P., Lafleur, P. M., Lee, H., Mazhitova, G., Nelson, F. E., Rinke, A., Romanovsky, V. E., Shiklomanov, N., Tarnocai, C., Venevsky, S., Vogel, J. G., and Zimov, S. A.: Vulnerability of Permafrost Carbon to Climate Change: Implications for the Global Carbon Cycle, BioScience, 58(8), 701–714, doi:10.1641/B580807, 2008.

Shibistova, O., Lloyd, J. O. N., Evgrafova, S., Savushkina, N., Zrazhevskaya, G., Arneth, A., Knohl, A., Kolle, O., and Schulze, E. D.: Seasonal and spatial variability in soil CO_2 efflux rates for a central Siberian Pinus sylvestris forest, Tellus B, 54(5), 552–567, doi:10.1034/j.1600-0889.2002.01348.x, 2002.

Stull, R. B.: An Introduction to Boundary Layer Meteorology, Kluwer Academic Punlishers, Dordrecht, 1988.

Sturm, P., Leuenberger, M., Sirignano, C., Neubert, R. E. M., Meijer, H. A. J., Langenfelds, R. L., Brand, W. A., and Tohjima, Y.: Permeation of atmospheric gases through polymer O-rings used in flasks for air sampling, J. Geophys. Res., 109, D04309, doi:10.1029/2003JD004073, 2004.

Styles, J. M., Lloyd, J. O. N., Zolotukhin, D., Lawton, K. A., Tchebakova, N., Francey, R. J., Arneth, A., Salamakho, D., Kolle, O., and Schulze, E. D.: Estimates of regional surface carbon dioxide exchange and carbon and oxygen isotope discrimination during photosynthesis from concentration profiles in the atmospheric boundary layer, Tellus B, 54(5), 768–783, doi:10.1034/j.1600-0889.2002.01336.x, 2002.

Tans, P. P., Fung, I. Y., and Takahashi, T.: Observational Constraints on the Global Atmospheric CO_2 Budget, Science, 247(4949), 1431–1438, doi:10.1126/science.247.4949.1431, 1990.

Tarnocai, C., Canadell, J. G., Schuur, E. A. G., Kuhry, P., Mazhitova, G., and Zimov, S.: Soil organic carbon pools in the northern circumpolar permafrost region, Global Biogeochem. Cy., 23, GB2023, doi:10.1029/2008gb003327, 2009.

Thompson, R. L., Manning, A. C., Gloor, E., Schultz, U., Seifert, T., Hänsel, F., Jordan, A., and Heimann, M.: In-situ measurements of oxygen, carbon monoxide and greenhouse gases from Ochsenkopf tall tower in Germany, Atmos. Meas. Tech., 2, 573–591, 2009, http://www.atmos-meas-tech.net/2/573/2009/.

Tohjima, Y., Katsumata, K., Morino, I., Mukai, H., Machida, T., Akama, I., Amari, T., and Tsunogai, U.: Theoretical and experimental evaluation of the isotope effect of NDIR analyzer on atmospheric CO_2 measurement, J. Geophys. Res.-Atmos., 114, D13302, doi:10.1029/2009JD011734, 2009.

Trusilova, K., Rödenbeck, C., Gerbig, C., and Heimann, M.: Technical Note: A new coupled system for global-to-regional downscaling of CO2 concentration estimation, Atmos. Chem. Phys. Discuss., 9, 23187–23210, 2009, http://www.atmos-chem-phys-discuss.net/9/23187/2009/.

Valentini, R., Dore, S., Marchi, G., Mollicone, D., Panfyorov, M., Rebmann, C., Kolle, O., and Schulze, E. D.: Carbon and water exchanges of two contrasting central Siberia landscape types: regenerating forest and bog, Funct. Ecol., 14(1), 87–96, doi:10.1046/j.1365-2435.2000.00396.x, 2000.

Vermeulen, A. T.: CHIOTTO Final Report, ECN energy research Centre of the Netherlands, 2007.

Vivchar, A. V., Moiseenko, K. B., Shumskii, R. A., and Skorokhod, A. I.: Identifying anthropogenic sources of nitrogen oxide emissions from calculations of Lagrangian trajectories and the observational data from a tall tower in Siberia during the spring-summer period of 2007, Izv. Atmos. Oceanic Phys., 45(3), 302–313, doi:10.1134/S0001433809030049, 2009.

Winderlich, J.: Entwicklung und Test eines Probenahme- und Kalibriersystems für einen kontinuierlich messenden Hochpräzisions-CO2-Analysator zum Einsatz in kommerziellen Flugzeugen (engl: Development and Test of a Sample Conditioning and Calibration System for a High Accuracy Continuous CO_2 Analyzer for Deployment in Commercial Aircrafts), Diploma thesis, Physikalisch-Astronomische Fakultaet, Friedrich Schiller University, Jena, 84 pp., 2007.

Zhao, C. L. and Tans, P. P.: Estimating uncertainty of the WMO mole fraction scale for carbon dioxide in air, J. Geophys. Res., 111, D08S09, doi:10.1029/2005JD006003, 2006.

Table 1. Part list of ZOTTO setup.

Element	Company	Type	Symbol
inlets	Solberg Filter, Continental Industrie GmbH, Germany	F-15-100	I1-6
filters 40 µm	Swagelok, BEST Fluidsysteme GmbH, Germany	SS-12TF-MM-LE and SS-8F-K4-40	F1-6
filters 2 µm	Swagelok, BEST Fluidsysteme GmbH, Germany	SS-4FW-2	F7-13
flushing pumps	Gardner Denver Thomas GmbH, Germany	617CD32	CF1-6
purge pump	KNF Neuberger GmbH, Germany	N86KNE	CP1
3-way solenoid valves	Gems Sensors GmbH, Germany	G3415-LC-24VDC-VAC	V1-8
12 position multiport valve	Valco Instruments Company Inc. from Machery-Nagel GmbH & Co. KG, Germany	EMTMA-CE	VA1
needle valves	Hy-Lok D Vertriebs GmbH, Germany	NV3H-12M-R	NV1-6
needle valves	Swagelok, BEST Fluidsysteme GmbH, Germany	SS-4MG SS-SS4	NV7-8 NV9-11
needle valves	Swagelok, BEST Fluidsysteme GmbH, Germany	SS-2MG	NV12-18
flow meters 0–20 l/min	Sensortechnics GmbH, Germany	FTAL020NU	FM1-6
flow meter 0–500 ml/min	MKS Instruments Deutschland GmbH, Germany	179B52CS3BM	FM7
flow meter 0–1000 sccm	Sensortechnics GmbH, Germany	FBAL001DU	FM8-14
pressure sensor 0-1 bara	Sensortechnics GmbH, Germany	CTE8001AK0	P1-7
pressure sensor 0-210 bar	Synotech Sensor und Meßtechnik GmbH, Germany	GCT-2251210BGC42C06	P8-11
pressure regulator	Tescom Europe GmbH & CO. KG, Germany	64-344XKA412-S	RE1-4
laboratory temperature and converter	Electrotherm GmbH, Germany LKM electronic GmbH, Germany	K6S-E-4LS-200C-G1/4A-120 and LKM-214	not shown

Table 2. CO_2 and CH_4 concentrations of calibration and target gases.

Tank name	ID number	CO_2 [ppm]	CH_4 [ppb]
Calibration Tank 1	D478665	354.71±0.08	1804.73±1.60
Calibration Tank 2	D436606	394.60±0.06	1899.26±1.49
Calibration Tank 3	D436607	453.12±0.08	2296.69±2.05
Target Tank	D478666	404.40±0.08	1947.43±1.37

Table 3. Meteorological instrument types and locations at ZOTTO.

Instrument	Company	Type	Tower	Bare land	Forest
Wind: 3-D ultrasonic-anemometer	Gill Instruments, UK	1210R3-50	4, 52, 92, 158, 227, 301 m a.g.l.	–	–
Air temperature and rel. humidity sensor	MELA Sensortechnik GmbH, GER	KPK1_6- ME-H38	4, 52, 92, 158, 227, 301 m a.g.l.	–	–
Air pressure transmitter	R.M.Young, USA	61204V	4, 92, 301 m a.g.l.	–	–
Radiation fluxes net radiometer	Kipp & Zonen B.V., NED	CNR1	301 m a.g.l.	–	–
2× Photosynthetically active radiation sensors	Kipp & Zonen B.V., NED	PAR Lite	301 m a.g.l.	–	–
3× Soil heat flux plates	McVan Instruments, Rimco, AUS	HP3/CN3	–	Both sites at −0.03 m	
Soil temperature sensor	Jumo GmbH, GER	902830	–	Both sites at: −0.02, −0.04, −0.08, −0.16, −0.32, −0.64, −1.28 m	
Soil moisture probe	Delta-T Devices, UK	ML-2×	–	Both sites at: −0.08, −0.16, −0.32, −0.64, −1.28 m	
Photosynthetically active radiation sunshine sensor	Delta-T Devices, UK	BF3H	–	2 m	–
Precipitation: tipping bucket rain gauge (heated)	Adolf Thies GmbH, GER	5.4032. 35.009	–	2 m	–

AMTD
3, 1399–1437, 2010

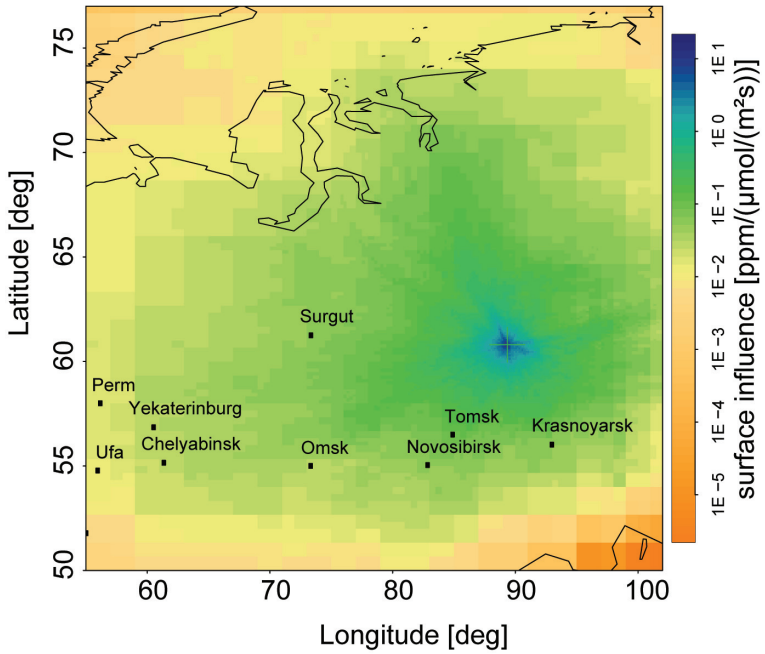

Fig. 1. STILT footprint for ZOTTO made from 5 days back trajectories from 1 May–30 November 2009.

AMTD
3, 1399–1437, 2010

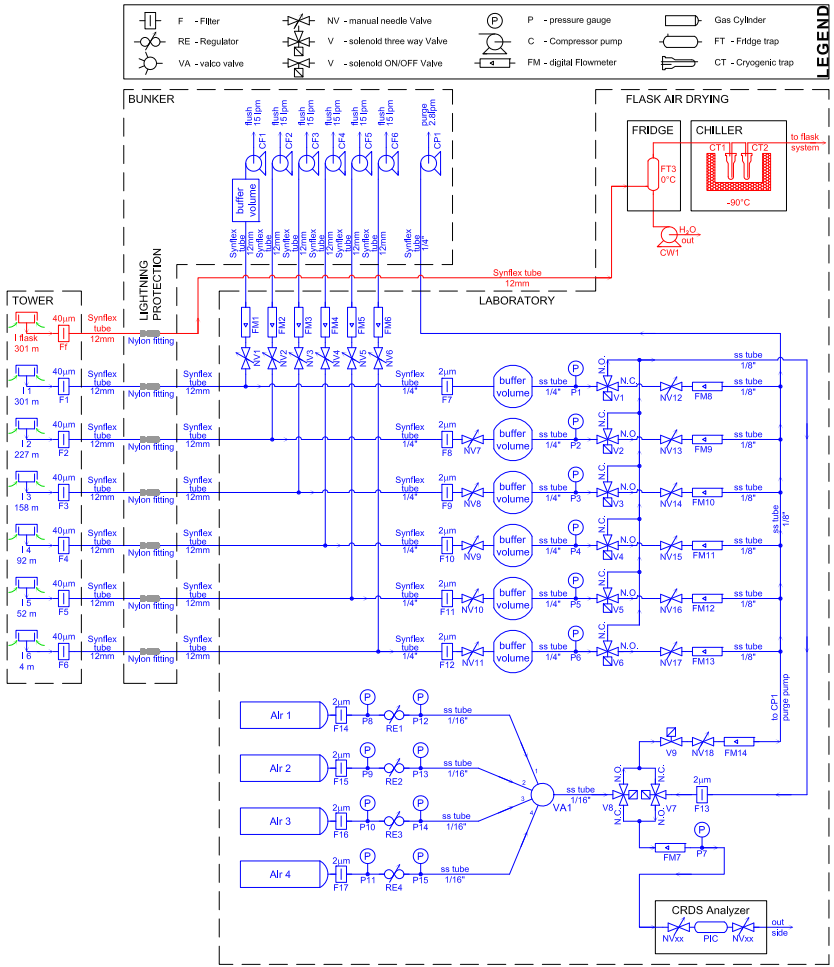

Fig. 2. Flow diagram of the CO_2/CH_4 measurement system at ZOTTO.

AMTD
3, 1399–1437, 2010

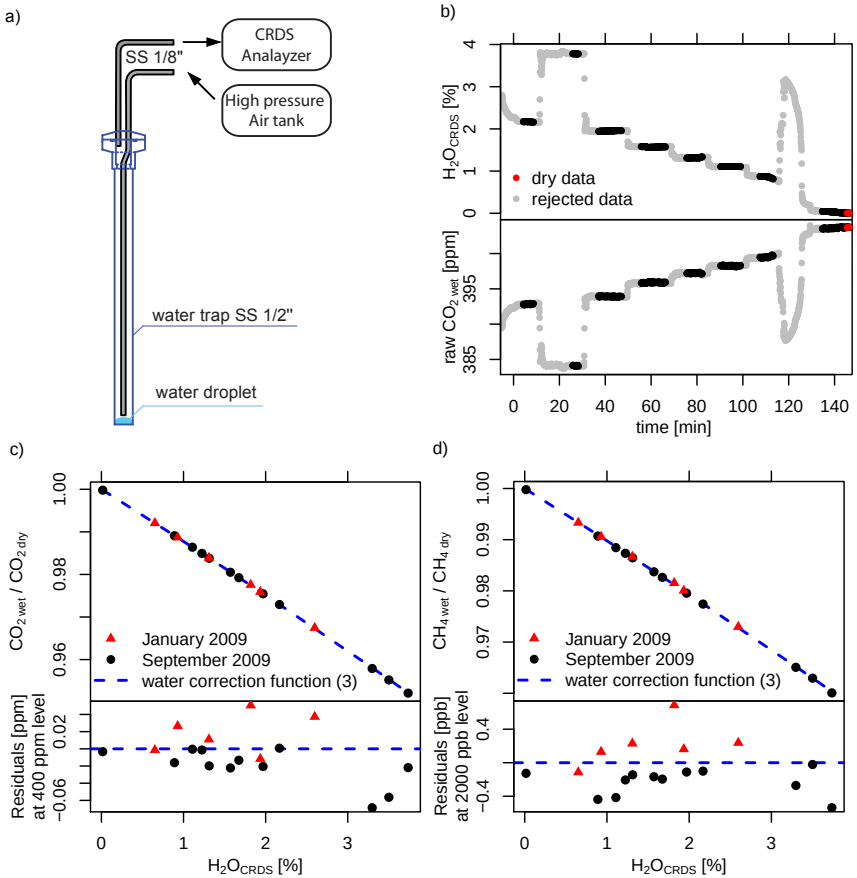

Fig. 3. Experiments at various water vapor levels: **(a)** setup; **(b)** H_2O and CO_2 time series of an experiment in September 2009; correction function derived from all experiments for **(c)** CO_2 and **(d)** CH_4.

AMTD
3, 1399–1437, 2010

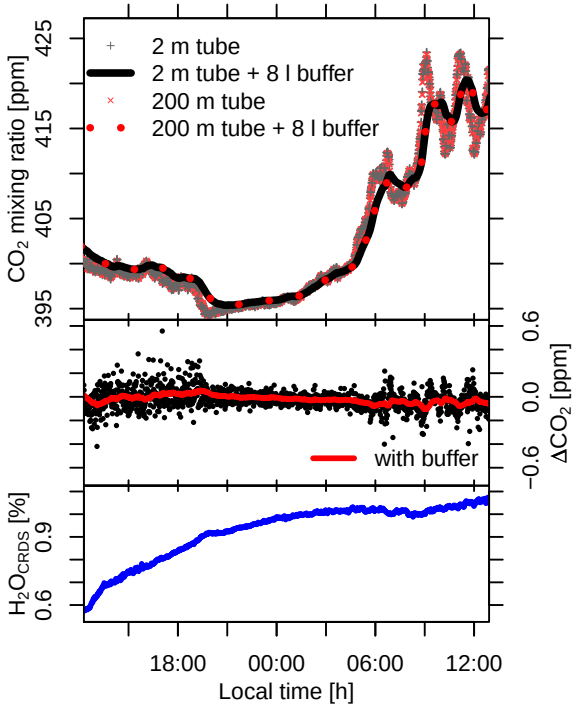

Fig. 4. Comparison of CO_2 measurement through 200 m and 2 m wet tubes (only a subset of data shown).

AMTD
3, 1399–1437, 2010

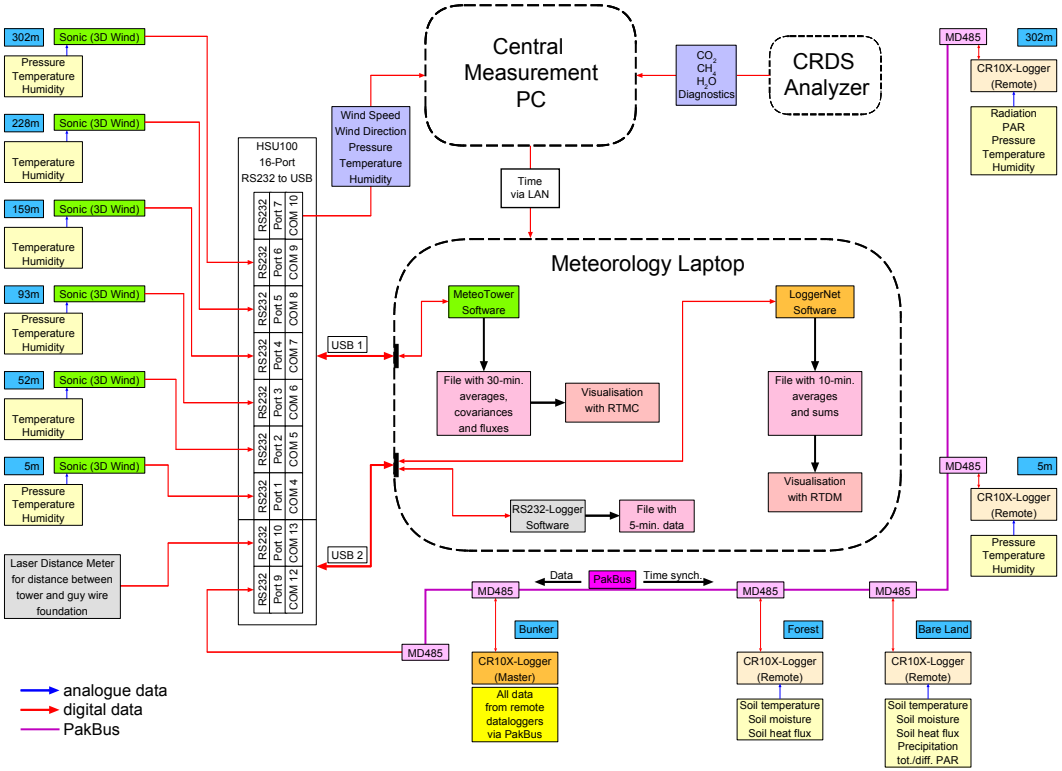

Fig. 5. Scheme of the meteorological measurement setup, the data handling and data distribution.

AMTD
3, 1399–1437, 2010

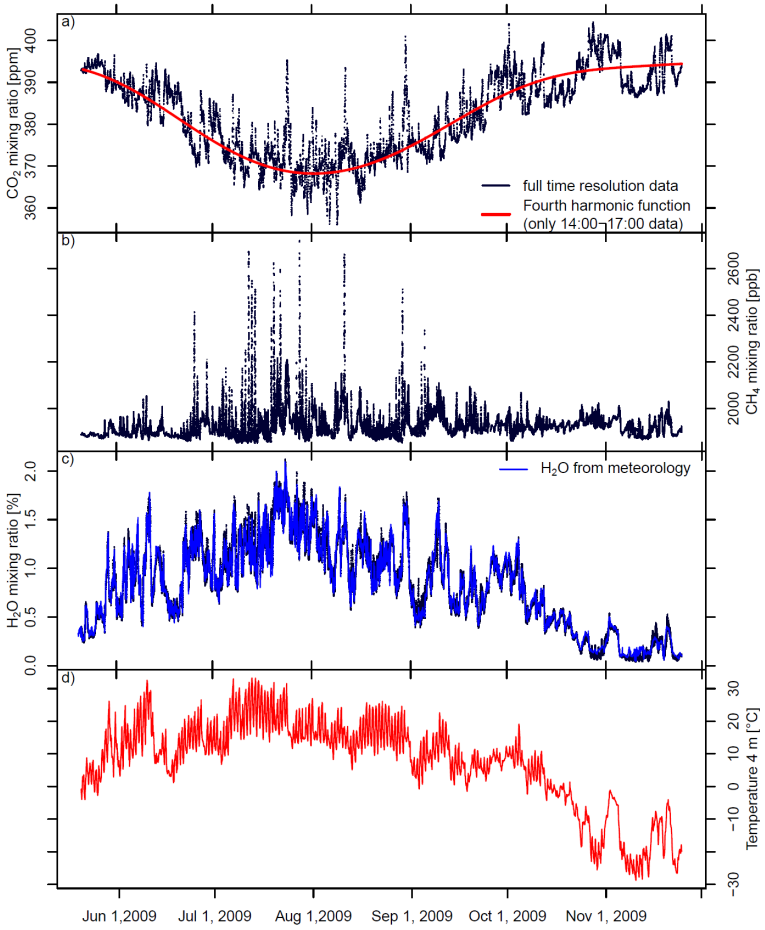

Fig. 6. ZOTTO time series for **(a)** CO_2, **(b)** CH_4, and **(c)** H_2O for 301 m height; **(d)** temperature.

AMTD
3, 1399–1437, 2010

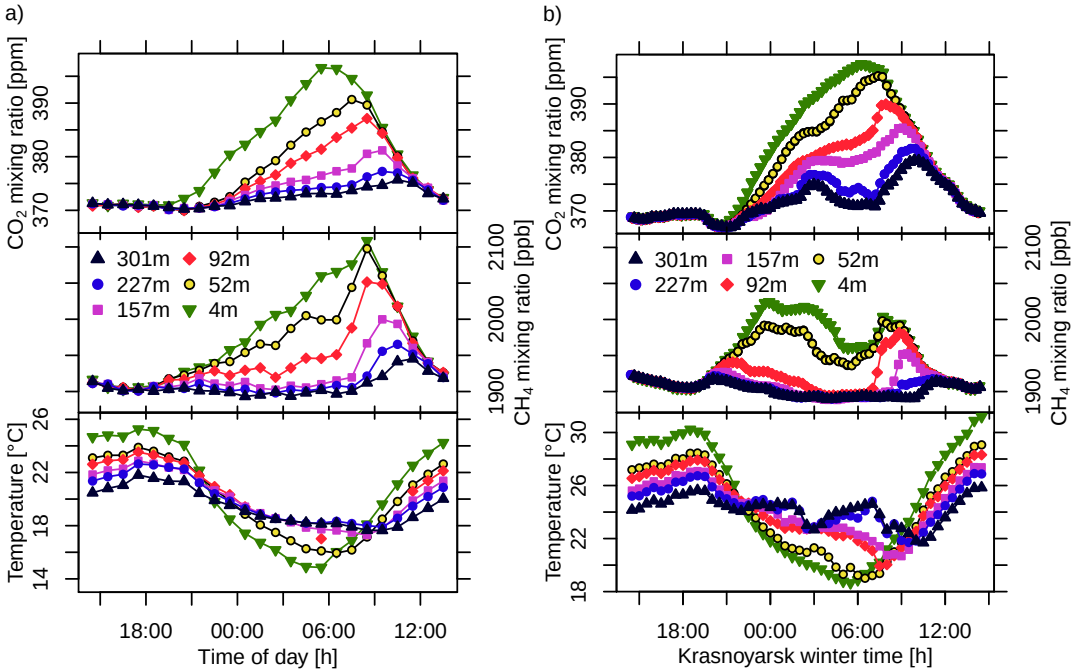

Fig. 7. ZOTTO time series from 6 tower heights for CO_2, CH_4, and temperature: **(a)** average July 2009; **(b)** from 22 to 23 July 2009.

AMTD
3, 1399–1437, 2010